

UHF RFID Tag Antenna Using Meander Patch for Metallic Object

#Ching-Han Tsai, Horng-Dean Chen, Yu-Hung Tsao
Dept. of Optoelectronics and Communications Engineering,
National Kaohsiung Normal University
No.62, Shenzhong Rd., Kaohsiung County 824, Taiwan
belldandys_fan@yahoo.com.tw, hdchen@nknuc.nknu.edu.tw

I. Introduction

The use of radio frequency identification (RFID) system has increased noticeably in recent years. The tag antenna has been particularly influential in the performance of RFID system. Many applications require tag antennas to be of low profile mounted on electrically metallic objects. Several designs have been developed for RFID patch-type antennas or planar inverted-F antennas (PIFAs) mountable on metallic objects [1]–[4]. Although most of these reported antennas can give the required reading-range performance, they may suffer from inconvenient mounting on metallic object because of their high profile. However, it is inherent for a patch-type antenna that lowering the antenna profile would degrade its radiation efficiency and antenna gain. Hence, an effort is being made to further improve the antenna gain of the low-profile patch antenna needed to provide the applicable reading range in a RFID application.

In this paper, we propose novel designs of low-profile meandered patch antennas suitable for UHF band RFID tags mountable on metallic objects. In this design, a long patch is bent to several half-wavelength radiating elements, which makes the surface currents of all radiating elements in phase and thus achieves an enhanced gain. Furthermore, it is shown that higher gain is obtained by an increased number of radiating elements. The details of the proposed designs and obtained experimental results are presented and discussed.

2. Antenna Design

Figs. 1(b), 1(c), and 1(d) show the proposed three meandered patch antennas, where the patches are bent to two, three, and four elements, respectively. The dimensions given in the figures are for operating in the 902 to 928 MHz frequency band. All the antennas are printed on very thin FR4 substrates with thickness of 0.8 mm, dielectric constant of 4.4. Note that the elements 1 (A to B) of all the meandered patches are linearly tapered, and its width t and length ℓ are selected so that complex impedance matching between the antenna and tag chip can be achieved. The elements 2 (B to C), 3 (C to D), and 4 (D to E) are all designed to have an effective length of about 0.5 wavelength at 915 MHz. Since the path of each of elements is 0.5 wavelength and produces a 180° phase shift of the element current, the exciting currents on all the elements (elements 1 ~ 4) are in the same direction, leading to an enhanced antenna gain in the $\theta = 0$ direction. The tag chip, which is attached to a plastic strap with metallic pads, is placed between the termination A of the element 1 and the ground plane through a shorting pin. To verify the gain-enhanced characteristic, a reference antenna that has an approximate half-wavelength patch structure is compared to the proposed meandered patch antennas, and its design parameters are shown in Fig. 1(a).

3. Results and discussions

The tag chip used in this design is Alien Higgs in strap package, which exhibits an impedance of $13 - j111 \Omega$ at the frequency of 915 MHz. In order to deliver maximum power between the chip and antenna, the input impedance of the antenna needs to be $13 + j111 \Omega$ at 915 MHz. First, we consider the design of the impedance matching for the four-element antenna. To

obtain the desired impedance value, two adjustable parameters are the width t and length ℓ of the element 1. Fig. 2 shows the measured input impedance as a function of width t with the parameter of $\ell = 73$ mm. It is first noted that for the case of $t = 5$ mm, the reactance curve never passes through 111Ω at all. This implies that the matching goal cannot be achieved for $t = 5$ mm. By decreasing the width t , the input reactance is increased. When the width t is decreased to 0.2 mm, the input impedance of $14 + j111 \Omega$ is obtained but occurred at 895 MHz. Furthermore, the parameter of $t = 0.2$ mm was fixed, and the influence of varying the length ℓ on the input impedance was examined and presented in Fig. 3. It is found that when the length ℓ decreases, the impedance curve is almost unchanged but shifted to higher frequency. At the length of $\ell = 67$ mm, the antenna has an input impedance of $13 + j112 \Omega$ at 915 MHz. This completes the conjugate impedance matching between the antenna and the chip.

Fig. 4 presents the measured return loss of the two, three, four-element antennas and reference antenna in free space. The corresponding bandwidth performances are given in Table I. It is seen that all the antennas are well matched with chip impedance. Their impedance bandwidths, determined from 10-dB return loss, are about 12 ~ 14 MHz. Also note that for achieving the impedance matching, the width t of the element 1 needs to be decreased when an increased element is added to the antenna. It is found that it is difficult for the antenna with more than four elements to achieve a matching condition. Good agreement between the measurement and simulation (obtained from the software Ansoft HFSS) is observed. The effect of an electrical metal platform on the tag antenna performance was studied. It is found that the operating frequency and the impedance characteristics of all the antennas are insignificantly affected by varying the metal-plate size.

Table I: Antenna performances in free space and on the 400×400 mm² metal plate for the antennas studied in Fig. 4. The Bandwidth is determined with 10-dB return loss.

	Bandwidth (MHz)		Simulated maximum gain (dBi)		Measured and calculated reading ranges (m)	
	Free space	Metal plate	Free space	Metal plate	Free space	Metal plate
Reference antenna	909–921	911–923	−9.6	−11.4	2.2, 2.6	1.6, 2.2
Two-element	906–918	904–917	−8.1	−9.3	2.8, 3.1	2.3, 2.8
Three-element	908–920	909–921	−7.0	−7.9	3.4, 3.5	2.7, 3.3
Four-element	905–919	904–919	−6.1	−6.8	4.2, 4.1	3.4, 3.7

The simulated radiation patterns are presented in this study. Fig. 5 shows the simulated co-polarization radiation patterns at 915 MHz for all four antennas placed in free space (without metal plate) and on the 400×400 mm² metal plate, where all the field components are normalized by the maximum value of the four-element case. It is seen that for all the antennas, the main beam maximum occurs in the $\theta = 0$ direction and does not vary with the size of the metal plate. The back radiation in the $-z$ direction is decreased when the antenna is mounted on the metal plate. It is also found that the addition of more radiating elements provides significant increase in antenna gain. About 3.5 dB improvement in the antenna gain is obtained for the four-element antenna in free space, compared to the reference antenna. Table I shows the simulated maximum antenna gains, which occur at about 915 MHz for all the antennas. According to the simulated results, the antenna gain are low due to the low profile of antenna (antenna thickness of 0.8 mm or $0.0024\lambda_0$).

The reading range measurement of the fabricated tag was carried out in an open area. A commercial RFID reader (Symbol XR440) with the operating frequency of 902–928 MHz, output power of 30.0 dBm, and a circular polarized antenna gain of 6.0 dBi was used in the measurement. Table I lists the results of the measured and calculated reading ranges for all four antennas placed in

free space and on the $400 \times 400 \text{ mm}^2$ copper plate. The calculated reading range was obtained by using Friis transmission formula. As shown, the measured reading ranges are consistent with the calculated values. It is also seen that the reading range significantly increases with the increase in the number of the radiating elements. The reading range of the four-element tag antenna in free space reaches 4.2 m and is about 2 m longer than that of the reference antenna. This is a simple verification of the gain enhancement of the proposed meandered patch antenna compared to the reference antenna. Furthermore, when the proposed antennas are attached to a large metal plate, they give a slight degradation in the reading-range performance. From the results obtained, it can be inferred that the proposed meandered patch antennas are suitable for various applications requiring identification of metallic objects.

4. Conclusions

Novel low-profile meandered patch antennas with various radiating elements have been successfully implemented. Results demonstrate that the reading ranges larger than 4 m can be obtained for the proposed antennas placed in free space. No severe degradation in the reading range is observed for the antennas mounted on a large metal plate.

Acknowledgments

This work is sponsored by the Institute of Antenna Engineering Taiwan.

References

- [1] H. Kwon, B. Lee, "Compact slotted planar inverted-F RFID tag mountable on metallic objects," *Electron. Lett.*, vol. 41, pp. 1308–1310, 2005.
- [2] Y. Um, U. Kim, J. Choi, "Design of a compact CPW-fed UHF RFID tag antenna for metallic objects," *Microwave Opt. Technol. Lett.*, vol. 50, no. 5, pp. 1439–1443, 2008.
- [3] S.L. Chen, K.H. Lin, "A slim RFID tag antenna design for metallic object applications," *IEEE Antennas Wireless Propagat. Lett.*, vol. 7, pp. 729–732, 2008.
- [4] H.D. Chen, Y.H. Taso, "Low-Profile PIFA Array Antennas for UHF Band RFID Tags Mountable on Metallic Objects," *IEEE Trans. Antennas Propagat.*, vol. 58, no. 4, pp. 1087–1092, 2010.

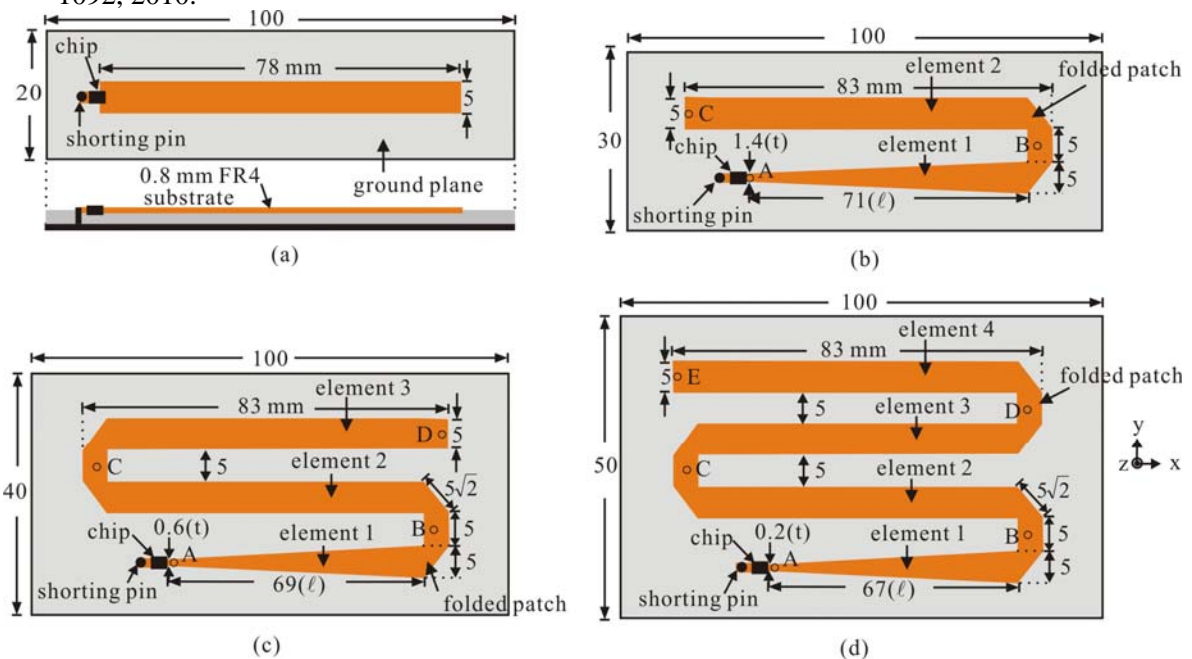


Fig. 1 Geometries of the proposed meandered patch antennas. (a) One element (reference antenna). (b) Two elements. (c) Three elements. (d) Four elements.

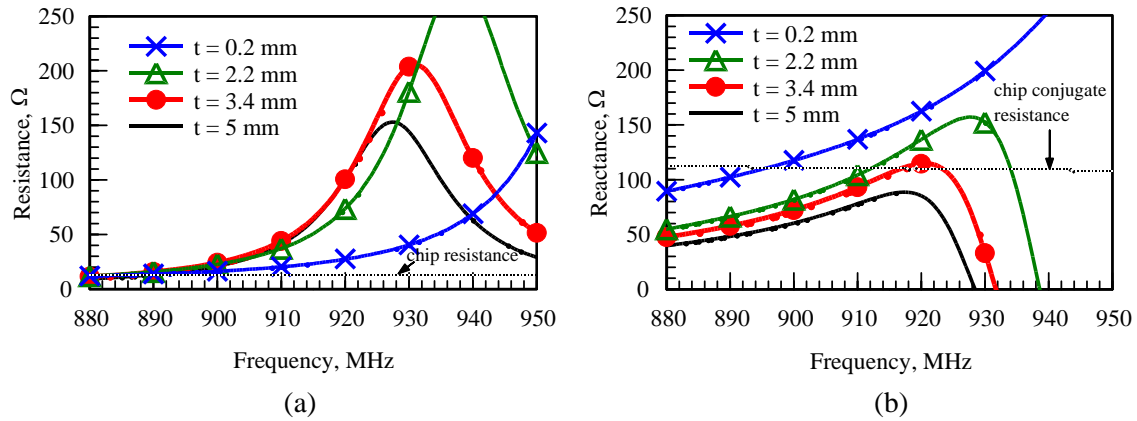


Fig. 2 Measured input impedance for the four-element patch antenna with various widths t ; $\ell = 73$ mm. Other parameters are shown in Fig. 1(d). (a) Input resistance. (b) Input reactance.

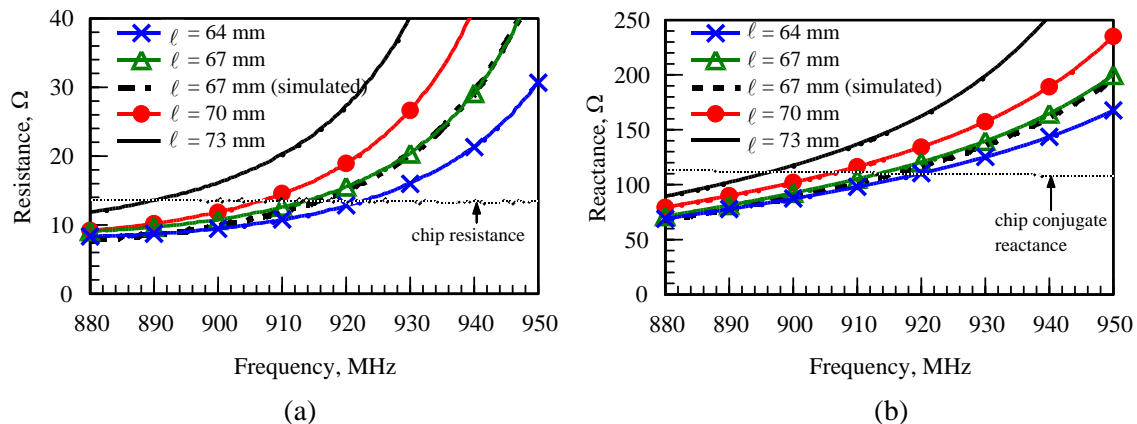


Fig. 3 Measured and simulated input impedance for the four-element meandered patch antenna with various lengths ℓ ; $t = 0.2$ mm. Other parameters are shown in Fig. 1(d). (a) Input resistance. (b) Input reactance.

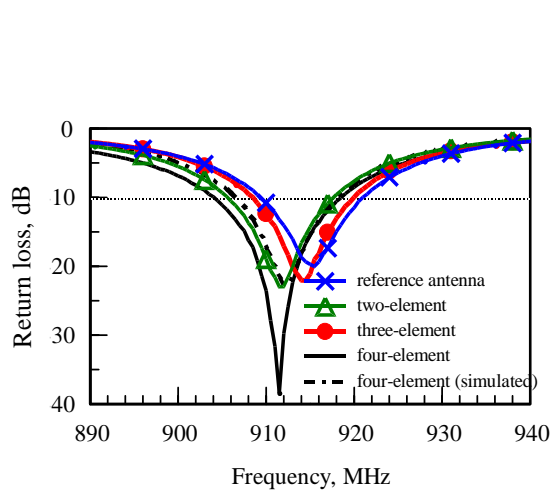


Fig. 4 Measured and simulated return loss for three meandered patch antennas and reference antenna in free space. Two-element: $t = 1.4$ mm and $\ell = 71$ mm. Three-element: $t = 0.6$ mm and $\ell = 69$ mm. Four-element: $t = 0.2$ mm and $\ell = 67$ mm. Other parameters are shown in Fig. 1.

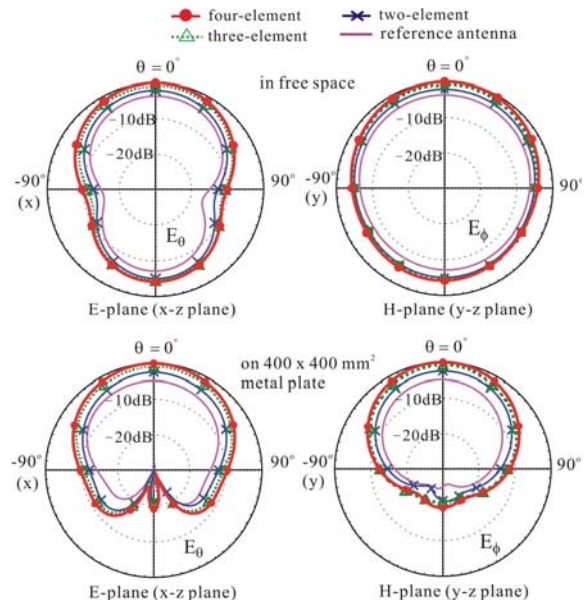


Fig. 5 Simulated radiation patterns at 915 MHz in free space and on a 400×400 mm² metal plate for the antennas studied in Fig. 4.